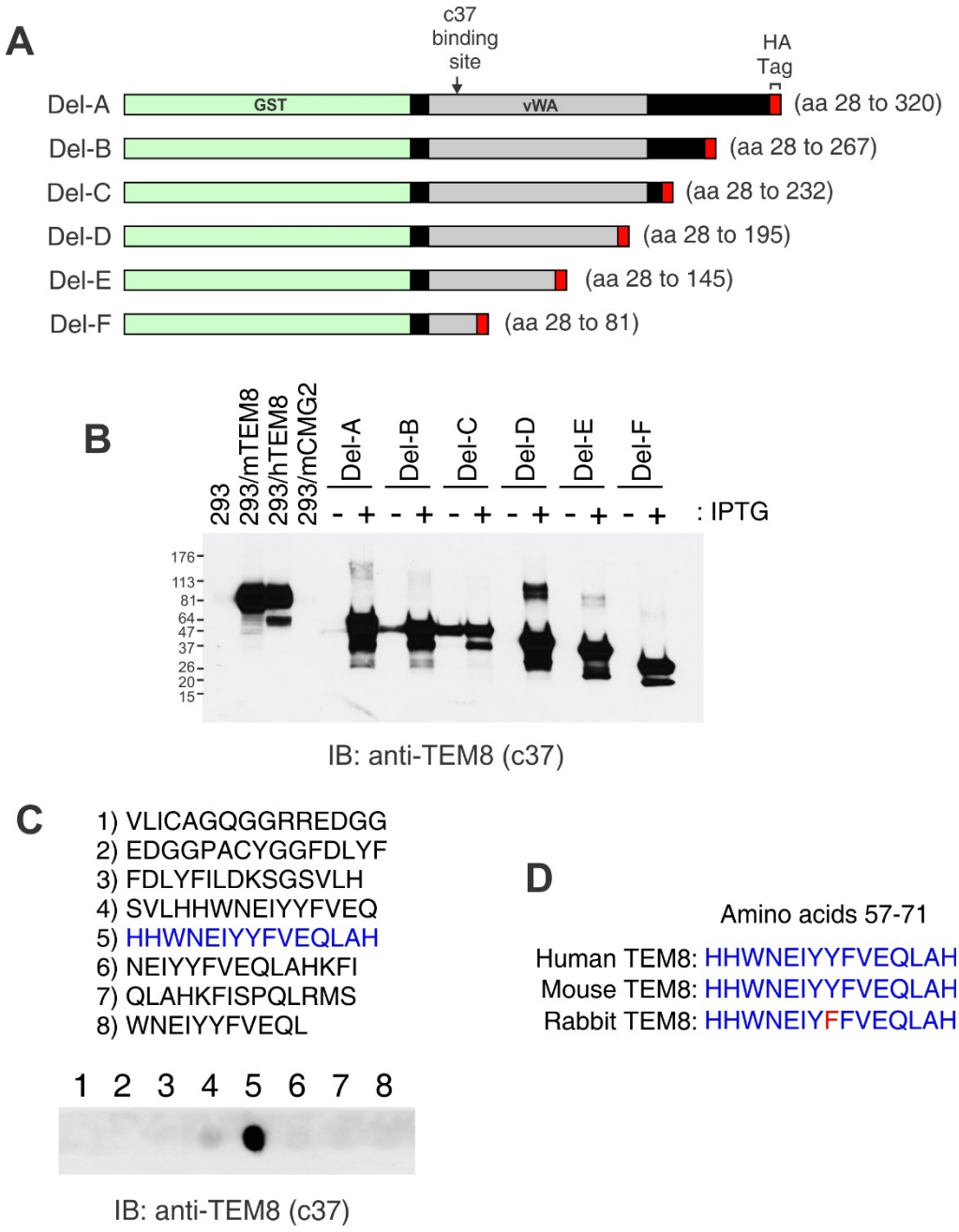

Supplemental Figure 1. Epitope mapping reveals c37 mAb binds near the N-terminus of TEM8. (**A**) Schematic drawing of six GST-TEM8(ECD) deletion (Del) proteins. The c37 antibody binding site resides in the von Willebrand factor type A domain (vWA) near the N-terminus of TEM8. (**B**) TEM8-GST deletion proteins were separated by SDS-PAGE and immunoblotted (IB) using rabbit anti-TEM8 mAb (clone 37). 293 cells with or without TEM8 were included as positive and negative controls. (**C**) Immunoblot (dot blot) of eight TEM8 peptide sequences using rabbit anti-TEM8 mAb. The peptide showing the strongest reactivity is highlighted in blue. (**D**) 15-amino acid epitope binding region near the N-terminus of TEM8 that is 100% conserved between mouse and human, but differs by one amino acid with rabbit TEM8.

A

Summary of TEM8 IHC and IF staining of tissue microarrays				
	Normal		Tumor	
	no. pos	% pos	no. pos	% pos
IHC				
breast	0/30	0	20/34	59
colon	0/8	0	25/29	86
esophageal	0/5	0	8/9	89
kidney	2*/22	9	66/79	84
lung	0/41	0	125/166	75
ovarian	0/10	0	37/59	63
pancreatic	0/44	0	79/117	68
uterus	0/12	0	42/70	60
IF				
breast	0/3	0	17/17	100

B

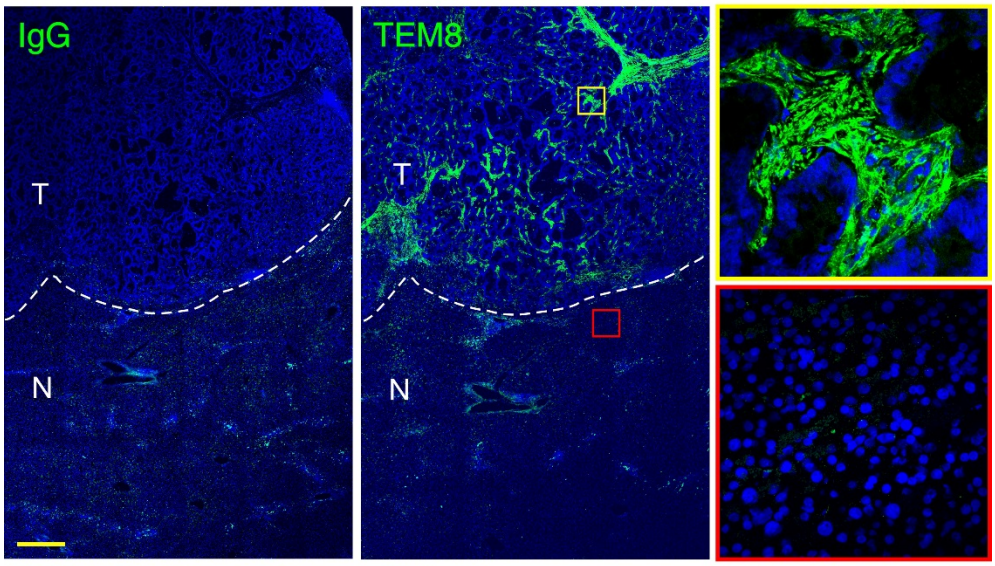

C

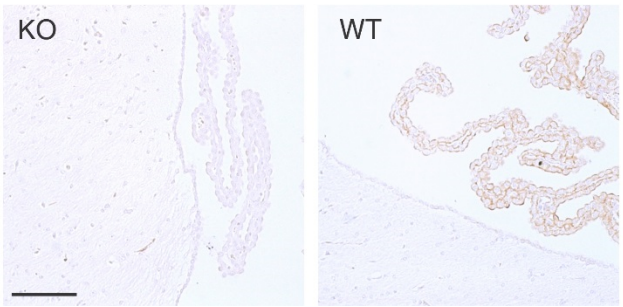

Supplemental Figure 2. TEM8 displays widespread expression in tumor associated stroma. (**A**) Table summarizing TEM8 immunohistochemistry (IHC) and immunofluorescence (IF) staining of tissue microarrays containing normal and tumor samples from 8 different tissue types. *Weak glomeruli staining was observed in two of the samples. (**B**) IF staining of normal (N)-tumor (T) margin of human colon cancer liver metastasis using rabbit anti-TEM8 mAb (green). Sections were counterstained with Hoechst 33258 nucleic acid stain (blue). Scale bar, 500 μm. (**C**) TEM8 IHC staining of choroid plexus epithelium in *Tem8* KO and WT mice using c37 rabbit anti-TEM8 mAb. Scale bar, 100 μm.

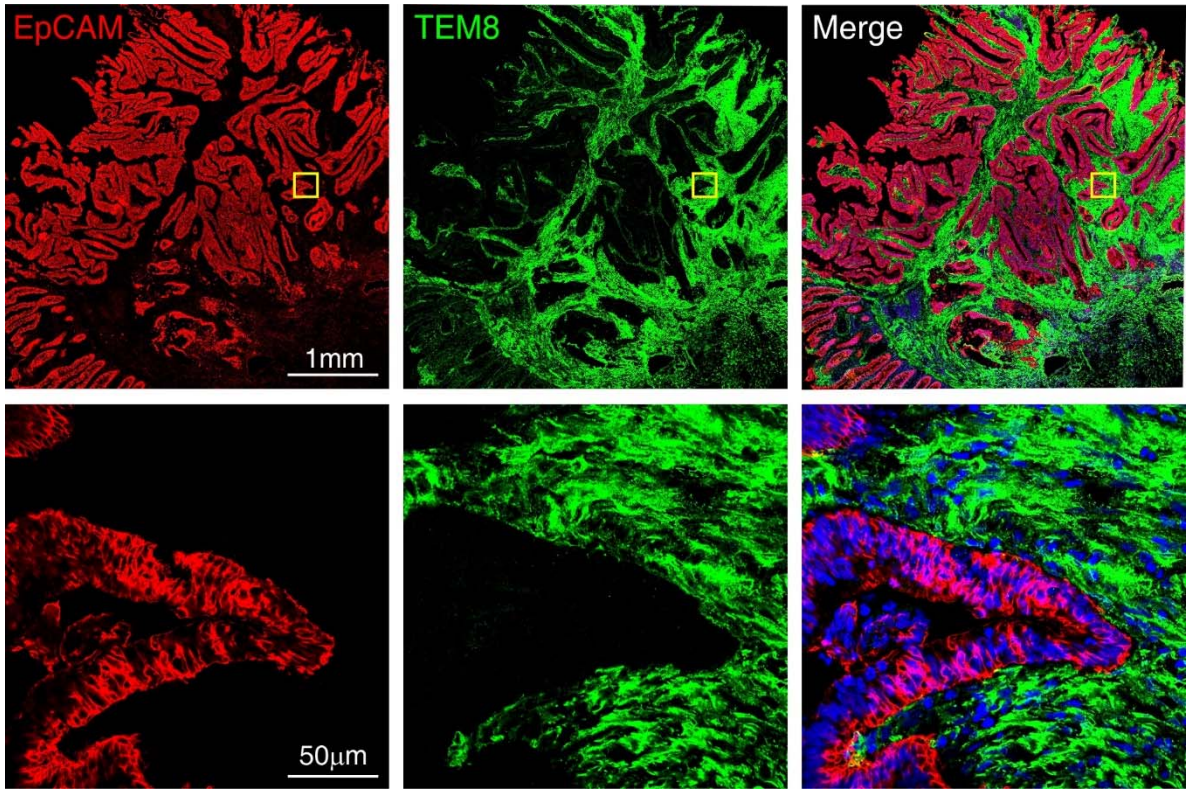

Supplemental Figure 3. TEM8 displays widespread expression throughout the tumor associated stroma. Immunofluorescence staining of human colon cancer using rabbit anti-TEM8 mAb (green) and mouse anti-EpCAM (red). The merged image also shows Hoechst 33258 nucleic acid stain (blue). Note TEM8 expression is predominantly in EpCAM-negative tumor-associated stroma.

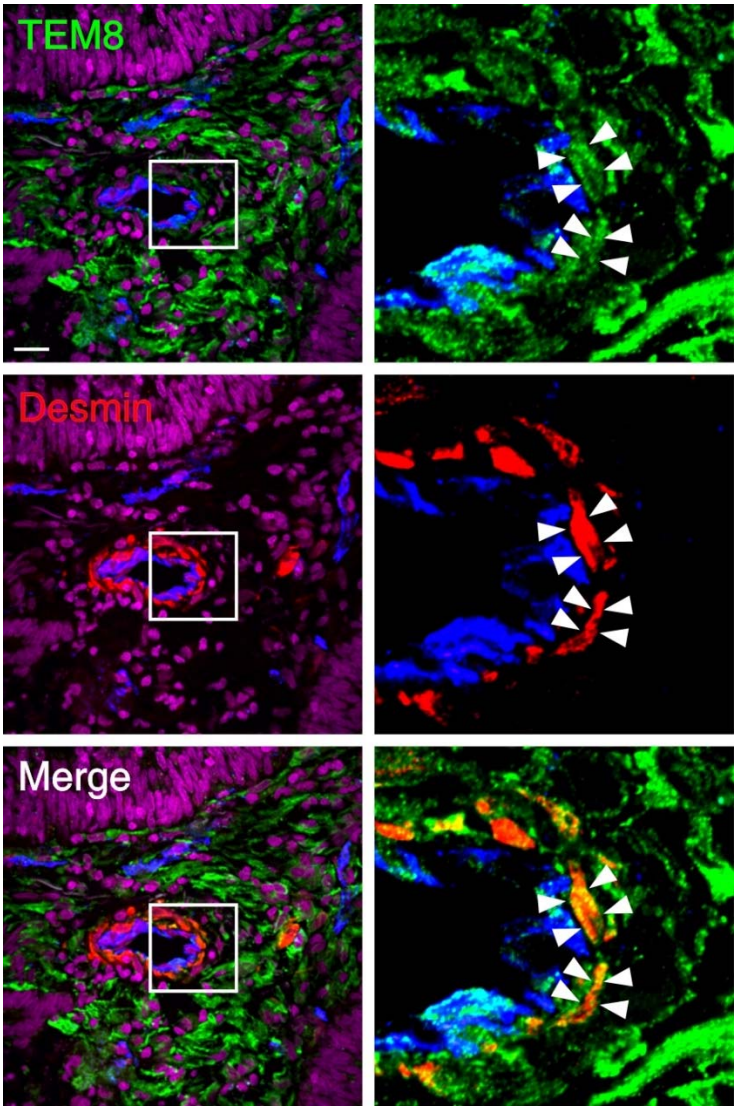

Supplemental Figure 4. TEM8 is found in tumor associated pericytes. Co-immunofluorescence staining of human colorectal tumors for TEM8 (green) and the pericyte marker desmin (red). TEM8-positive pericytes are highlighted (arrowheads). Vessels were labelled with CD31 antibodies (blue) and nuclei were stained with Hoechst 33258 (pseudocolored purple). Scale bar, 20 μm.

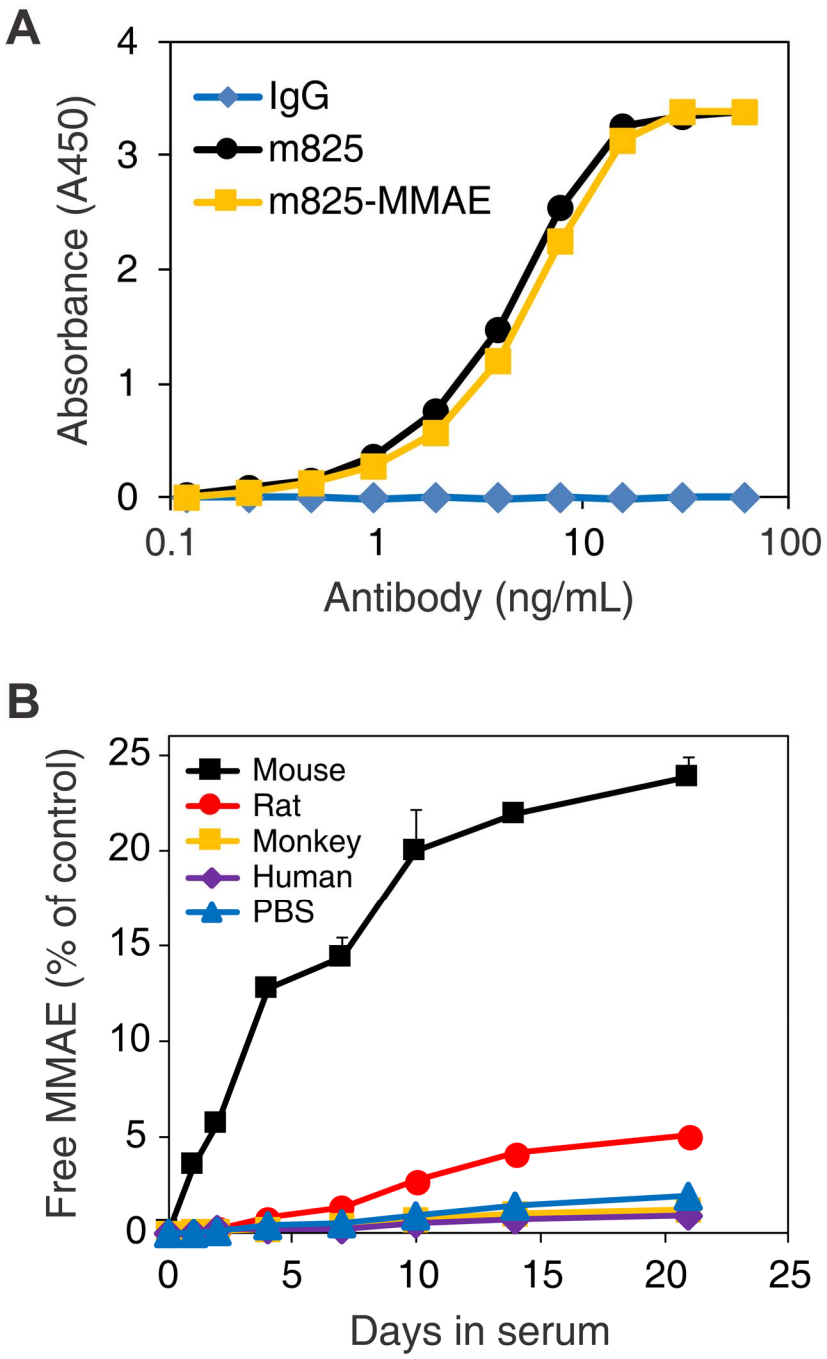

Supplemental Figure 5. m825-MMAE binds TEM8 and shows high stability in human serum. (**A**) ELISA demonstrates that m825 and the TEM8-ADC (m825-MMAE) both bind recombinant TEM8 extracellular domain. A non-specific IgG was used as a negative control. (**B**) Liquid chromatography-tandem mass spectrometry (LC-MS/MS) was used to evaluate TEM8-ADC stability in serum from various species. Data are means ± SD.

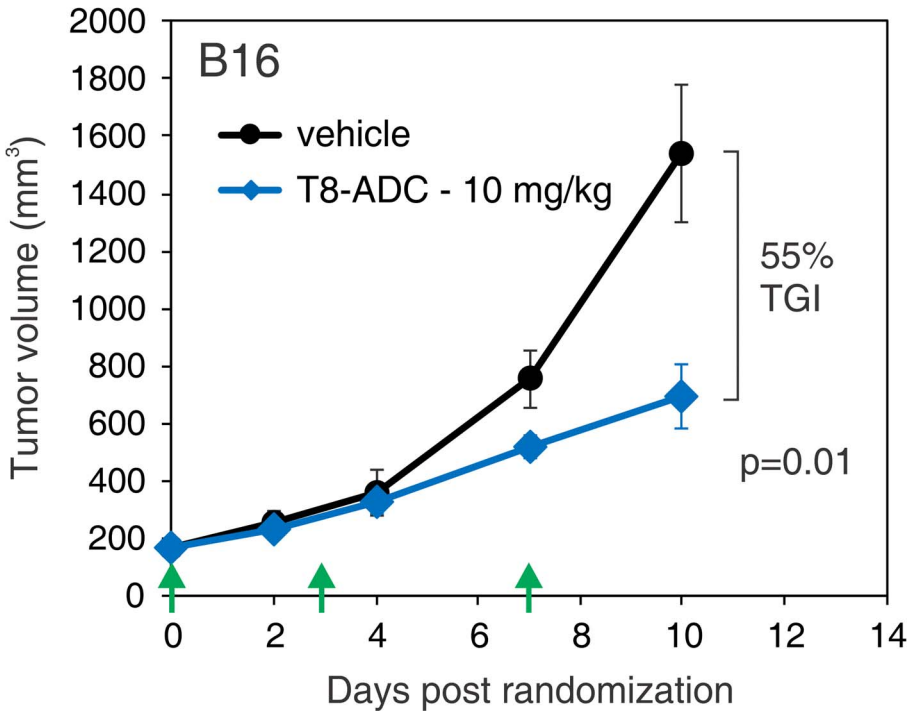

Supplemental Figure 6. B16 tumors display a moderate growth delay in response to TEM8-ADC treatment. Growth of subcutaneous mouse B16 melanoma tumors. Treatments with vehicle or m825-MMAE (T8-ADC) were initiated when tumors reached an average size of ~170 mm^3 and were administered on the days shown (green arrows). TGI = tumor growth inhibition. n = 8 (vehicle) or 9 (T8-ADC) per group. Data are means ± SEM.

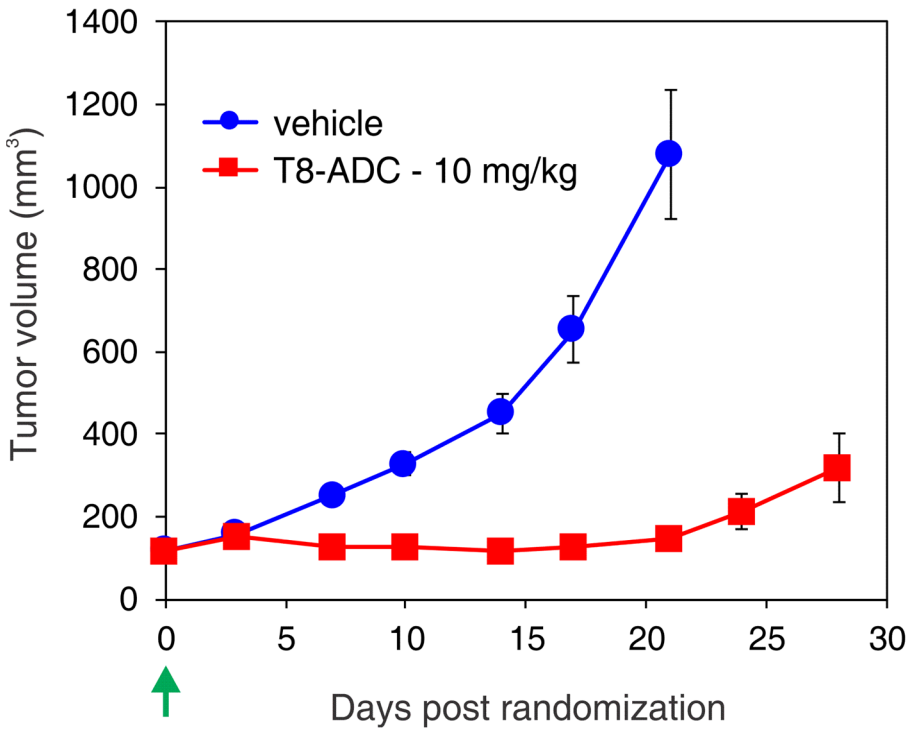

Supplemental Figure 7. Treatment with a single dose of m825-MMAE is sufficient to delay the growth of human breast tumor xenografts. A single treatment with vehicle or m825-MMAE (T8-ADC) was initiated when orthotopic MDA-MB-231 tumors reached an average size of ~100mm^3 (green arrow). n = 10 per group. Data are means ± SEM.

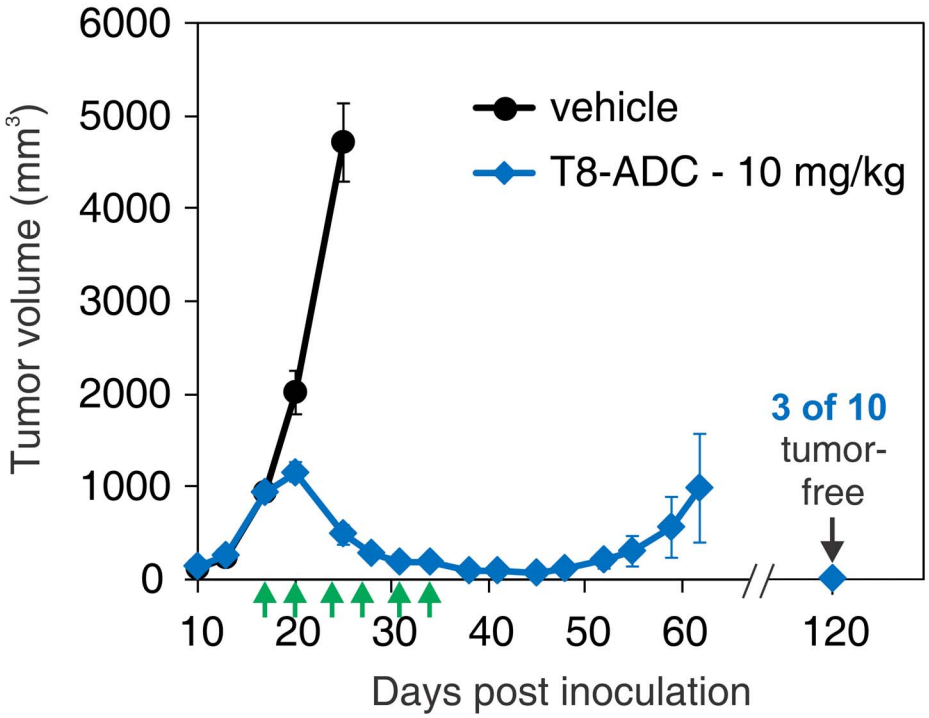

Supplemental Figure 8. m825-MMAE is effective against large COS-G PDX tumors. Growth of subcutaneous lung (COS-G) PDX tumors. Treatments with vehicle or m825-MMAE (T8-ADC) were initiated when tumors reached an average size of ~1000 mm^3 and were administered on the days shown (green arrows). n = 10 per group. Data are means ± SEM.

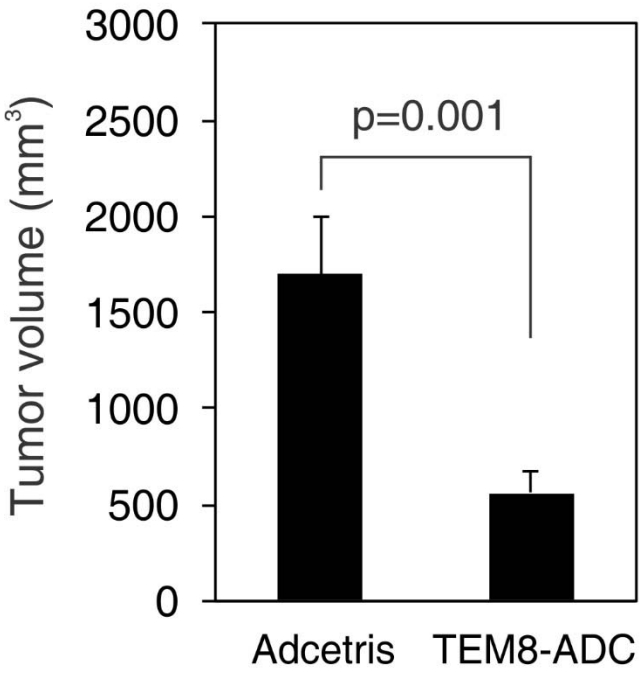

Supplemental Figure 9. TEM8-ADC shows specific anti-tumor activity in vivo. Growth of subcutaneous HT29 colon tumor xenografts. Treatments (biwk x 3) with a non-targeted ADC (Adcetris) or m825-MMAE (TEM8-ADC) were initiated when tumors reached an average size of ~100 mm^3 and tumor volume measured 6 weeks later. The Adcetris ADC uses the same drug-linker as TEM8-ADC. Adcetris binds human CD30 but does not show reactivity with HT29 cells or murine CD30. In this experiment n = 11 (Adcetris) or 13 (T8-ADC) per group. Data are means ± SEM.

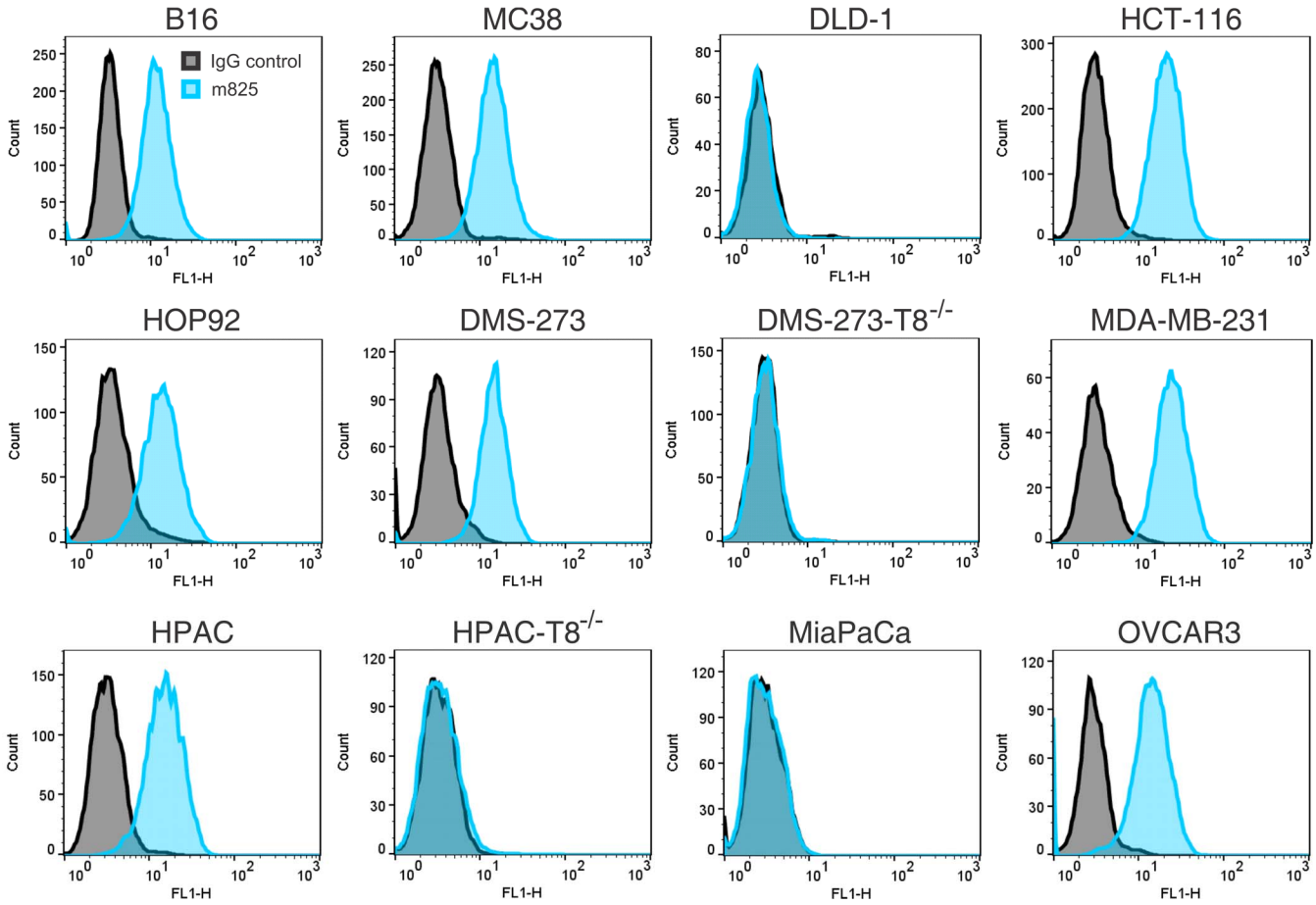

Supplemental Figure 10. TEM8 expression is detectable in some cancer cell lines. Flow cytometry was used to evaluate TEM8 expression in various mouse (B16 and MC38) and human (DLD-1, HCT116, HOP92, DMS-273, MDA-MB-231, HPAC, MiaPaCa and OVCAR) tumor cell lines using m825 and a non-specific isotype-matched human IgG control. Note the loss of m825 reactivity in DMS-273-T8$^{-/-}$ and HPAC-T8$^{-/-}$ cells following CRISPR-Cas9 mediated disruption of *Tem8*.

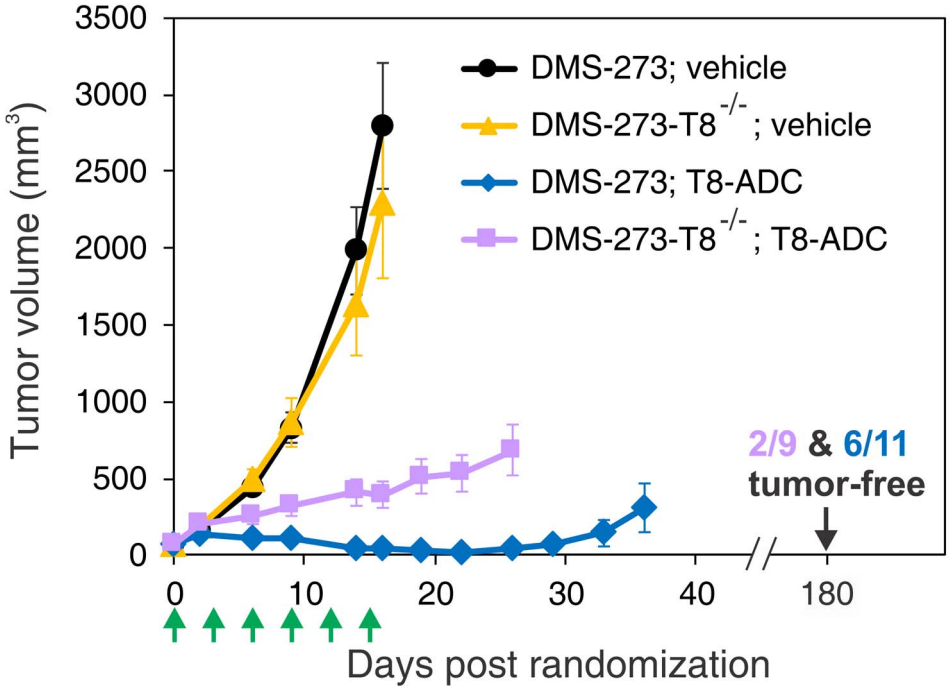

Supplemental Figure 11. TEM8 expression in tumor cells augments TEM8-ADC anti-tumor activity. Growth of subcutaneous human lung DMS-273 tumor xenografts following disruption of *Tem8* using CRISPR/Cas9 (DMS-273-T8$^{-/-}$). Treatments with vehicle or m825-MMAE (T8-ADC) were initiated when tumors reached an average size of ~100mm^3 and were administered on the days shown (green arrows). n = 10 to 12 per group. Data are means ± SEM.

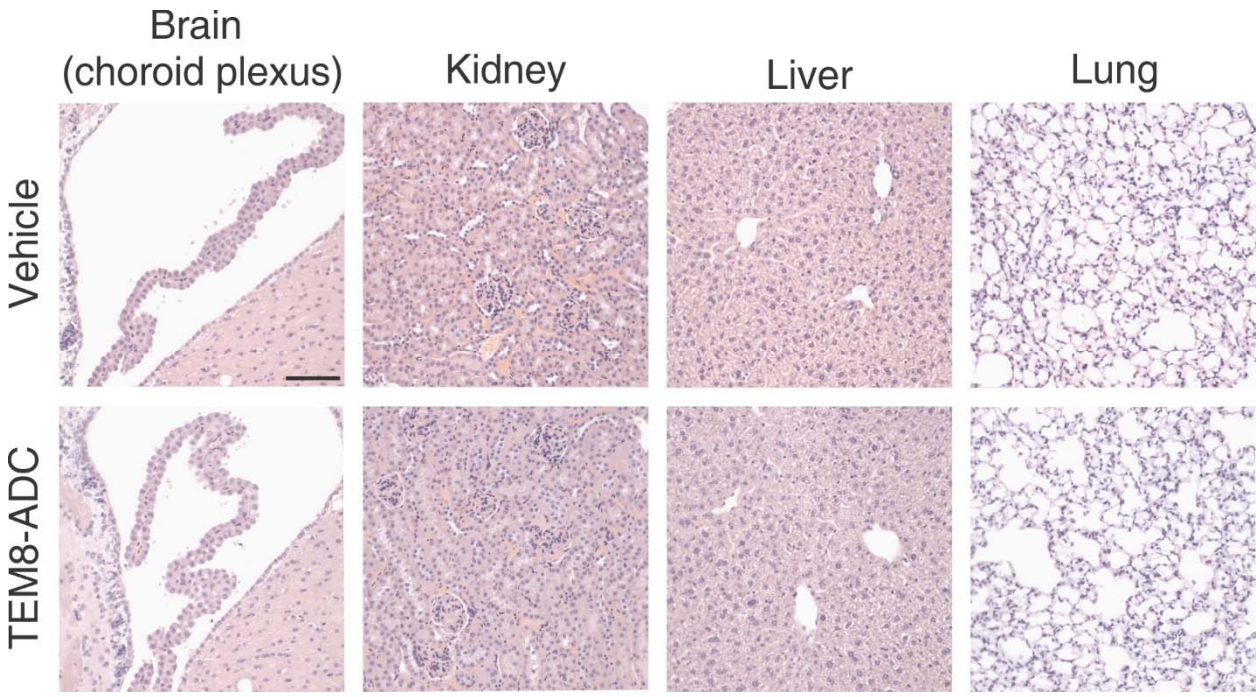

Supplemental Figure 12. TEM8-ADC is well tolerated in normal tissues. Mice were treated with vehicle (n=9) or 10 mg/kg of TEM8-ADC (n=9) 6 times (biwk x3) and tissues collected 24 h following the last treatment. No abnormalities were found in H&E stained sections of the adult brain (choroid plexus is shown), kidney, liver or lung. Scale bar, 100 μm.

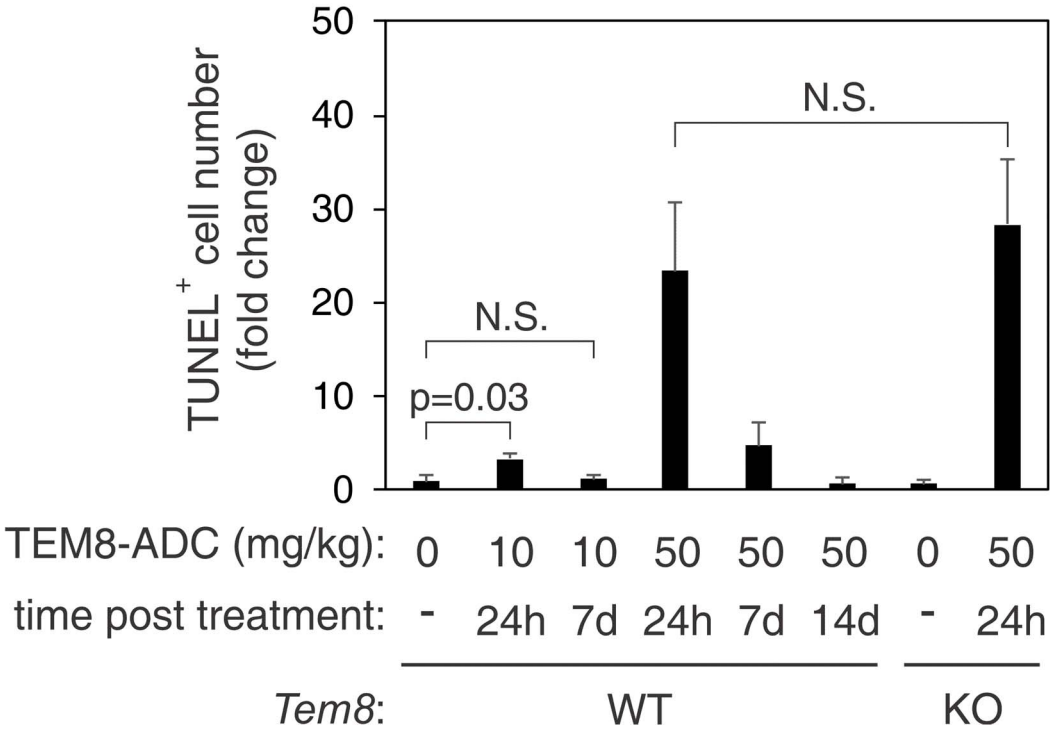

Supplemental Figure 13. TEM8-ADC treatment results in a transient increase in apoptosis in gastrointestinal cells. C57BL6 mice were treated with a single 10 or 50 mg/kg dose of TEM8-ADC and tissues were collected at 24 h, 7 days or 14 days post treatment and analyzed by TUNEL staining. The number of TUNEL positive cells was normalized to total Hoechst 33258 area and values displayed as fold change relative to the untreated control. n = 4 mice per group. Data are means ± SD. N.S.: Non-significant.

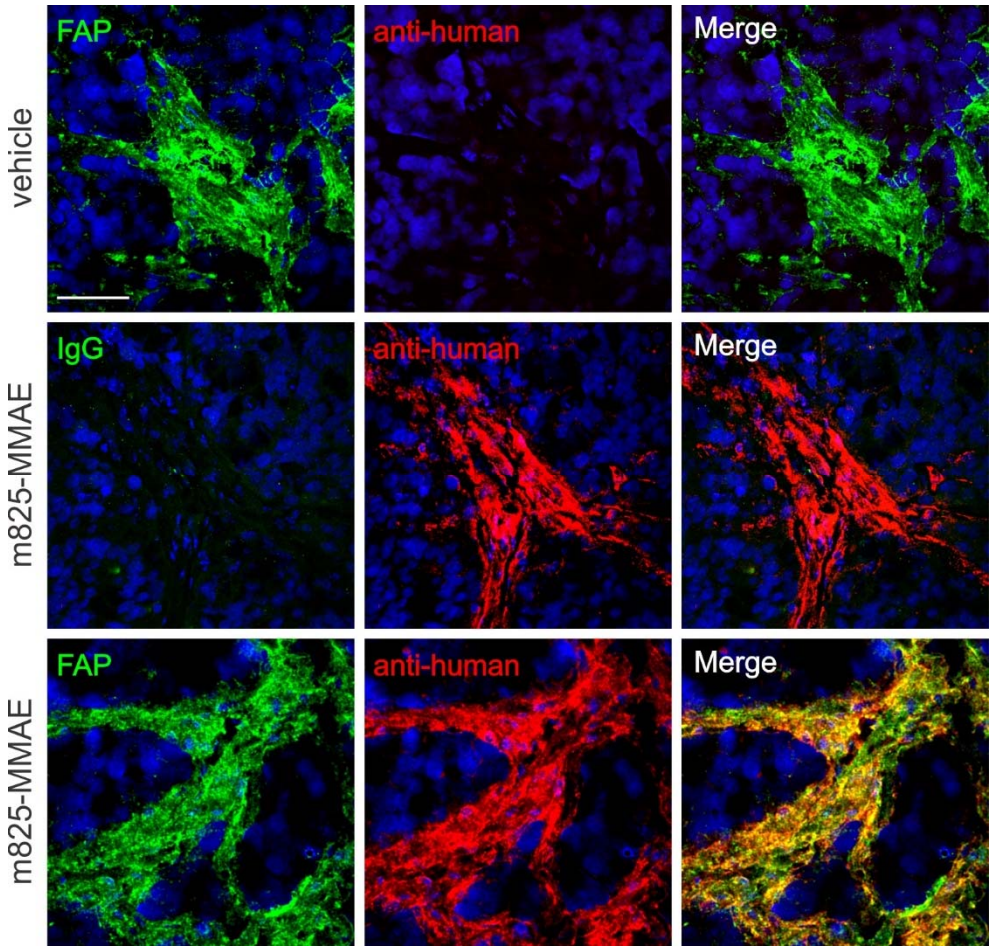

Supplemental Figure 14. Intravenously administered TEM8-ADC colocalizes with FAP. Co-immunofluorescence staining was used to monitor localization of m825-MMAE in HT29 tumors 24 hours post i.v. injection. The i.v injected m825-MMAE was detected by post-staining tissue sections with Texas Red-labelled donkey anti-human secondary antibodies (red). FAP was detected by staining with rabbit anti-FAP primary antibodies (green). Staining controls included vehicle treated HT29 tumors (top panel) and a non-specific isotype-matched rabbit IgG (middle panel). Note the co-localization of FAP and m825-MMAE (yellow) in the merged image (bottom panel). Sections were counterstained with Hoechst 33258 nucleic acid stain (blue). Scale bar, 50 μm.

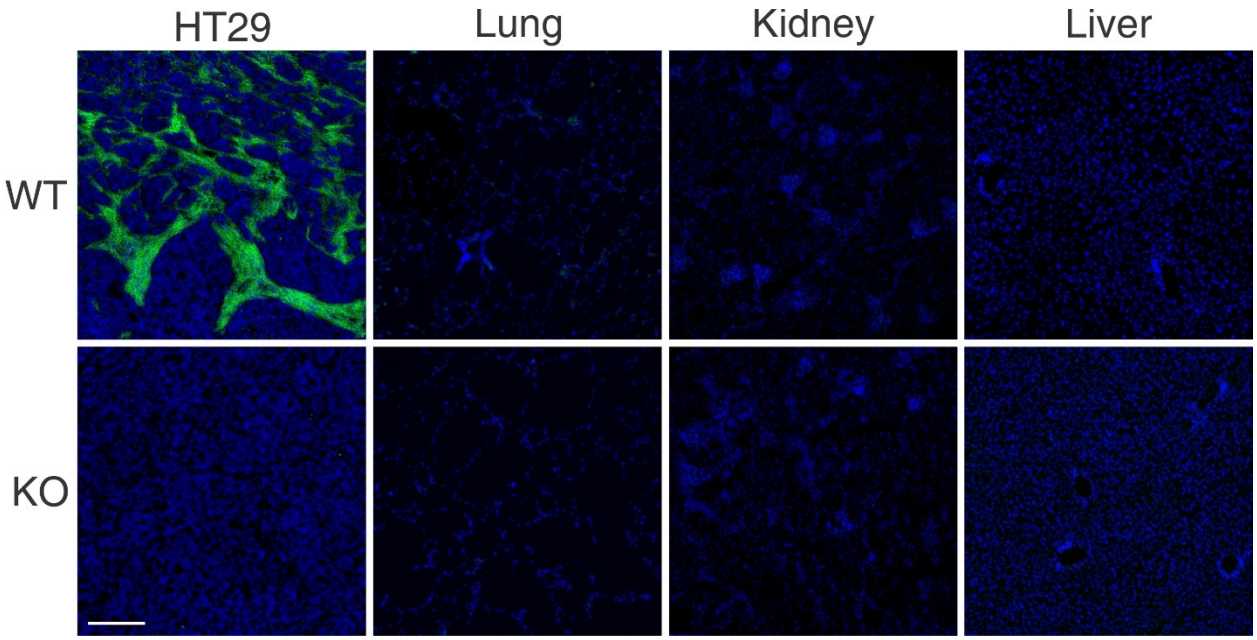

Supplemental Figure 15. Intravenously administered TEM8-ADC is not detectable in normal tissues. Immunofluorescence staining was used to monitor localization of m825-MMAE in HT29 tumors and normal tissues taken from TEM8 wildtype (WT) or knockout (KO) mice 24 hours post i.v. injection. To detect the i.v injected m825-MMAE, tissue sections were post-stained with FITC-labelled goat anti-human secondary antibodies (green). Sections were counterstained with Hoechst 33258 nucleic acid stain (blue). Scale bar, 200 μm.

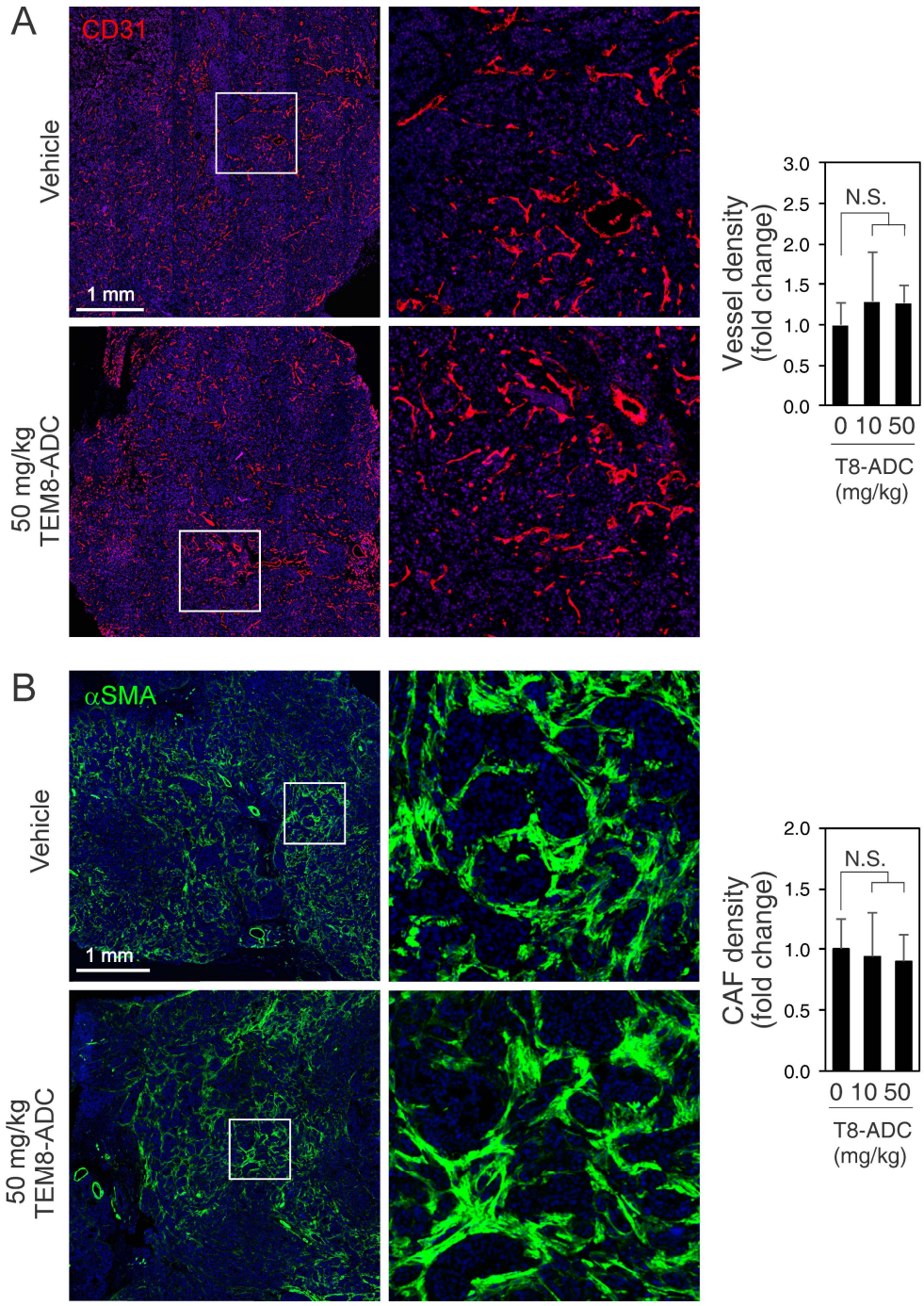

Supplemental Figure 16. TEM8-ADC does not alter CAF or vessel density. Immunofluorescence staining of orthotopic HPAC tumors for (**A**) CD31 (vessels) or (**B**) αSMA (CAFs) was performed 48 hours post treatment with vehicle (control), 10 or 50 mg/kg of TEM8-ADC. Representative tile scanned images along with higher resolution insets from the vehicle and 50 mg/kg groups are shown. Quantification of vessel and CAF density is shown on the right. Values represent fold change relative to the vehicle control. Data are means ± SD. N.S.: Non-significant.

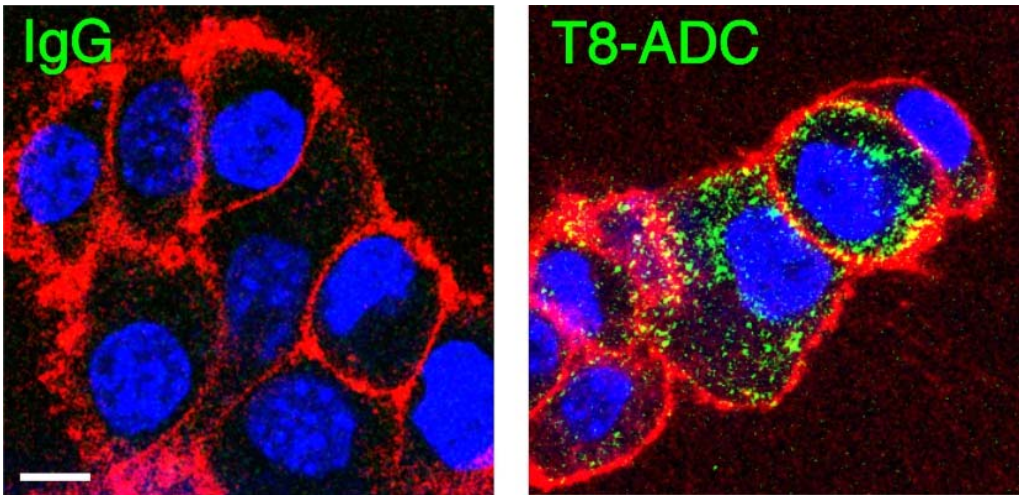

Supplemental Figure 17. TEM8-ADC is internalized in tumor stromal cells (TSCs). Uptake of the TEM8-ADC (green) was evaluated in TSCs after shifting cells from 4°C to 37°C for 60 minutes. A non-specific isotype-matched human IgG antibody was used as a negative control. Cells were counterstained with CellMask Orange plasma membrane stain (red) and Hoechst 33258 nucleic acid stain (blue). Scale bar, 10 μm.

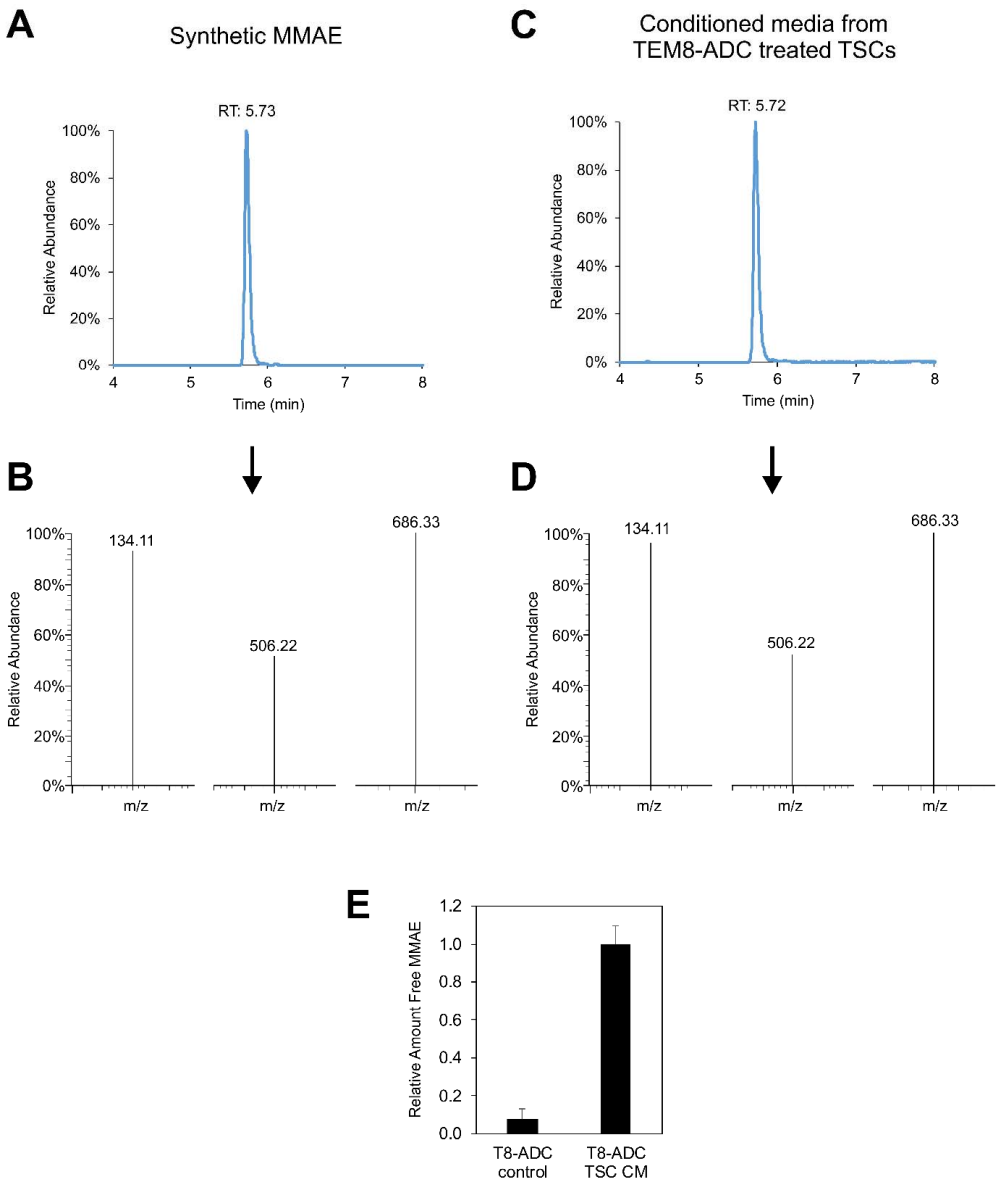

Supplemental Figure 18. Mass spectrometry (MS) identifies MMAE in the conditioned media of TEM8-ADC treated TSCs. (**A-D**) MS was used to evaluate the chromatographic retention time (A, C) and m/z fragment ion spectrum (B, D) of synthetic MMAE (A, B) and conditioned media from TEM8-ADC treated TSCs (C, D). The MMAE fragment ion spectrum was identical to synthetic MMAE indicating that the ADC was cleaved at the valine-citrulline dipeptide linker, resulting in the spontaneous intramolecular [1,6]-elimination of PABC and release of MMAE free-drug. (**E**) The relative amount of free MMAE detected by MS in conditioned media from TEM8-ADC treated TSCs and non-conditioned media containing TEM8-ADC. Data: means ± SD.

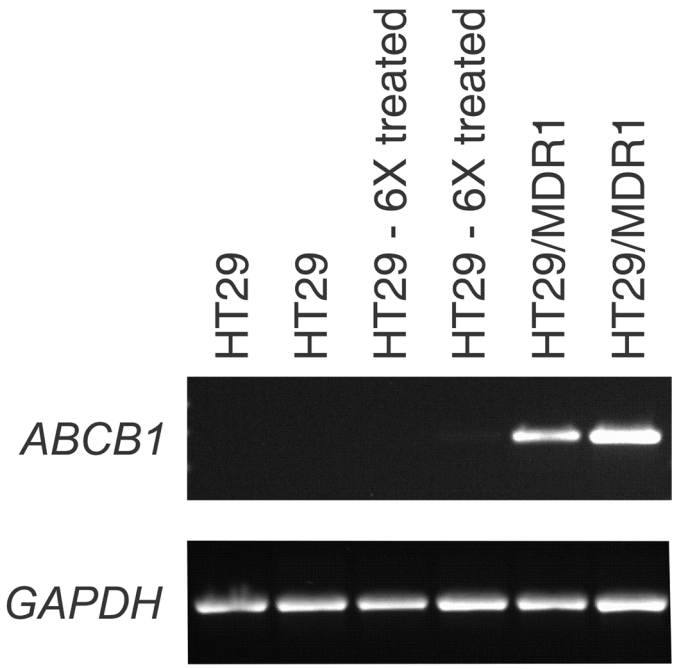

Supplemental Figure 19. RT-PCR was used to evaluate *ABCB1* mRNA expression in tumors following relapse. RT-PCR was used to evaluate human *P-gp* expression in tumor cells from untreated HT29 control tumors or HT29 tumors that had relapsed following 6 treatments with 10 mg/kg TEM8-ADC (biwk x 3). The RT-PCR primers were designed to span introns and react with human *ABCB1* but not mouse *Abcb1* coding sequences. Two independent tumors per group were assessed. HT29/MDR1 tumors were included as a positive control. As a loading control *GAPDH* was also amplified using human-specific primers.

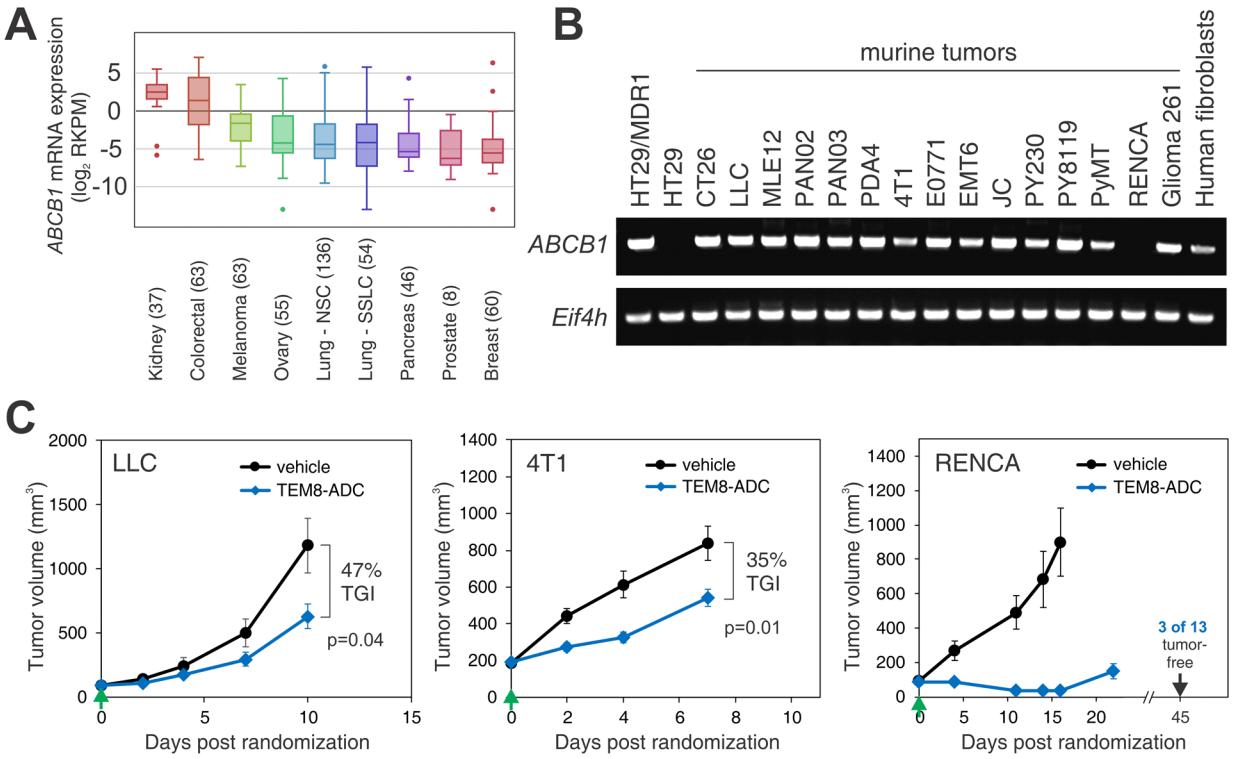

Supplemental Figure 20. P-gp expression predicts responsiveness to m825-MMAE. (**A**) Plot displaying relative *ABCB1* expression in human cancer cell lines derived from various tissues. The RNAseq data was obtained from the Cancer Cell Line Encyclopedia (CCLE). The horizontal line in the boxplots represents the median, outside points represent outliers, and the n in parenthesis indicates the number of cancer cell lines from each tissue. (**B**) RT-PCR (29 cycles) was used to evaluate *P-gp* expression in a panel of murine colon (CT26), lung (LLC, MLE-12), pancreatic (PAN02, PAN03, PDA4), breast (4T1, E0771, EMT6, JC, PY230, PY8119, PyMT), renal (RENCA) and brain (Glioma 261) tumors. The RT-PCR primers were designed to span introns and recognize regions of the *P-gp* coding sequence that are 100% conserved between human (*ABCB1*) and mouse (*Abcb1a* and *Abcb1b*). *P-gp* was also detected in primary human fibroblasts. *Eif4h* was included as a loading control, and primers were designed against regions of *Eif4h* that are 100% conserved between human and mouse. (**C**) Growth of murine subcutaneous LLC, orthotopic 4T1 and subcutaneous RENCA tumors. Treatments with vehicle or 10 mg/kg m825-MMAE (TEM8-ADC) were initiated when tumors reached an average size of ~100 to 200 mm^3 (green arrows) and administered twice per week. TGI = tumor growth inhibition. n = 7 (LLC), 14 and 15 (4T1) or 13 and 10 (RENCA) per group. Data are means ± SEM.

Supplemental Table 1. Selected Toxicological Results

	Chronic toxicity study:		Acute toxicity study:		
	vehicle	10 mg/kg TEM8-ADC biwk x 3	vehicle	10 mg/kg TEM8-ADC single dose	50 mg/kg TEM8-ADC single dose
White blood cells (K/ul)	7.1 ± 1.7	6.8 ± 1.2	5.7 ± 2.6	4.8 ± 0.4	5.1 ± 0.6
Neutrophil number (K/ul)	2.2 ± 0.4	2.0 ± 0.6	1.1 ± 0.5	1.0 ± 0.4	1.0 ± 0.3
Lymphocyte number (K/ul)	3.5 ± 0.9	3.1 ± 0.6	4.3 ± 2.1	3.5 ± 0.2	3.8 ± 0.6
Monocyte number (K/ul)	0.8 ± 0.1	0.8 ± 0.2	0.20 ± 0.03	0.18 ± 0.10	0.19 ± 0.05
Eosinophil number (K/ul)	0.5 ± 0.4	0.7 ± 0.5	0.11 ± 0.05	0.10 ± 0.07	0.12 ± 0.04
Basophil number (K/ul)	0.1 ± 0.1	0.2 ± 0.3	0.01 ± 0.01	0.02 ± 0.02	0.02 ± 0.01
Neutrophil (%)	31.7 ± 3.4	28.9 ± 5.0	18.8 ± 0.8	19.9 ± 6.0	19.5 ± 7.1
Lymphocyte (%)	49.4 ± 4.8	46.6 ± 10.2	75.4 ± 0.4	74.0 ± 8.9	74.1 ± 7.7
Monocyte (%)	11.8 ± 1.8	11.3 ± 2.7	3.8 ± 1.3	3.7 ± 1.8	3.7 ± 0.9
Eosinophil (%)	6.1 ± 3.7	10.3 ± 5.3	1.9 ± 0.1	2.0 ± 1.3	2.4 ± 0.6
Basophil (%)	1.0 ± 0.8	2.9 ± 3.0	0.2 ± 0.1	0.3 ± 0.4	0.3 ± 0.2
Red blood cells (M/uL)	10.1 ± 0.4	10.1 ± 0.5	10.0 ± 1.8	10.4 ± 0.5	10.5 ± 0.6
Hemoglobin (g/dL)	13.5 ± 0.4	13.8 ± 0.7	13.5 ± 2.0	14.3 ± 0.5	14.3 ± 0.6
Hematocrit (%)	43.7 ± 1.6	44.6 ± 2.1	49.8 ± 9.8	52.6 ± 1.6	53.7 ± 1.5
Mean cell volume (fL)	43.3 ± 0.4	44.0 ± 0.7	49.8 ± 1.1	50.6 ± 1.6	51.4 ± 1.7
Mean cell hemoglobin (Pg)	13.4 ± 0.6	13.6 ± 0.2	13.6 ± 0.4	13.8 ± 0.4	13.7 ± 0.5
Albumin (g/dL)	4.5 ± 0.1	4.5 ± 0.1	4.4 ± 0.4	4.2 ± 0.3	4.3 ± 0.2
Alkaline phosphatase (U/L)	169 ± 8	175 ± 19	170 ± 37	155 ± 21	161 ± 20.2
Alanine aminotransferase (U/L)	38.0 ± 1.6	37.0 ± 2.0	55.0 ± 19.8	48.5 ± 8.3	56.0 ± 12.4
Amylase (U/L)	798 ± 39	807 ± 72	1030 ± 23	935 ± 82	1126 ± 163
Total bilirubin (mg/dL)	0.4 ± 0.1	0.4 ± 0.1	0.4 ± 0.1	0.4 ± 0.1	0.4 ± 0.1
Calcium (mg/dL)	12.0 ± 0.4	12.2 ± 0.3	13.7 ± 0.8	13.0 ± 0.7	12.7 ± 0.4
Creatinine (mg/dL)	0.3 ± 0.1	0.2 ± 0.1	0.1 ± 0.1	0.2 ± 0.2	0.2 ± 0.2
Sodium (mmol/L)	147 ± 1	148 ± 4	154 ± 1	154 ± 3	153 ± 2.6
Potassium (mmol/L)	9.3 ± 0.6	9.3 ± 1.0	9.4 ± 0.8	10.1 ± 0.3	10.2 ± 0.5
Total protein (g/dL)	5.3 ± 0.1	5.7 ± 0.2	5.8 ± 0.1	5.8 ± 0.2	5.9 ± 0.2
Globulin (g/dL)	0.9 ± 0.1	1.3 ± 0.2	1.4 ± 0.4	1.6 ± 0.3	1.6 ± 0.4